Statistical properties of mesoscopic conductivity fluctuations in a short-channel GaAs field-effect transistor

A. O. Orlov, M. E. Raikh, I. M. Ruzin, and A. K. Savchenko

Institute of Radio Engineering and Electronics, USSR Academy of Sciences

(Submitted 15 June 1989)
Zh. Eksp. Teor. Fiz. **96**, 2172–2184 (December 1989)

We have investigated the distribution function for mesoscopic fluctuations in the hopping conductivity G which are observed in short-channel GaAs field-effect transistors as the gate voltage is varied. We show that the distribution function for $\ln G$ is asymmetrical and that it falls off smoothly for large values of G. This agrees with the results of theoretical studies of mesoscopic conductivity fluctuations for a system with exponential scatter in the values of its local conductivity. In order to describe the temperature dependence of the width of the distribution of $\ln G$ for the channel of a GaAs FET ($T = 1.5$ to 8 K), we propose a model for hopping conductivity in a short sample which takes into account short-range fluctuations in the charged donor potential.

1. INTRODUCTION

There have been several studies of mesoscopic fluctuations in the hopping conductivity of both one-dimensional[1,2] and two-dimensional[3,4] transistor structures as the electron concentration varies. In the first case a silicon MOS structure was investigated in which a narrow strip of n-type semiconductor with a width $\leqslant 1$ μm was defined by using acceptor doping. The conductivity of the strip was measured as current was passed along its long dimension. In the second case, the channel of a GaAs field-effect transistor was investigated. This channel also has the form of a strip; however, the conductivity is now measured along its short dimension. In this case, the explanation for the conductivity fluctuations which are observed as the voltage V_g at the Schottky gate varies is based on the idea that the conductivity of every sample is dominated by a small-area region where the conductivity is highest, whose resistivity in turn is determined by a single electron hop. The fluctuations in the conductivity G as V_g varies are related to shifts in the spatial location of this ("primary") hop which determines the conductivity across the entire sample. In Ref. 4 additional information was obtained: it was found that the crookedness of conductivity paths in the sample are small, and they are extended in the direction of the current. This was indicated by anisotropy of the magnetoresistance when the magnetic field was directed along and perpendicular to the direction of current, which clearly implies that the conducting paths can be pictured as consisting of resistors connected in series, each of which is associated with an electron hop between a pair of localized states.

The following question then arises: how is a particular conducting chain selected in a large-area sample? One possible explanation is the effect of fabrication inhomogeneity, as a result of which the effective width of the sample becomes much less than its geometric width. In this case the system becomes entirely equivalent to a one-dimensional system.[1]

Another possible explanation is related to the fact that because of strong scatter in the resistance associated with individual hops, even in a macroscopically homogeneous sample there will be certain paths which will be selected to carry the primary portion of the current through the sample. In this picture, exponentially widely-spaced and almost rectilinear chains of hops whose conductivity is anomalously large are responsible for the conductivity of a short sample. In a wide sample the probability of formation of such chains can be large.

A cardinal difference between these two explanations is the following: in the first case, the system consists of a set of series-connected high-impedance resistors, while in the second case low-impedance segments which join the contacts are responsible for the conductivity, and the total conductivity of the sample is determined by the sum of the inverse resistances of these portions. The central point of this article is the fact that an unambiguous choice can be made between these two alternative explanations by studying the statistics of the mesoscopic conductivity fluctuations in a single sample. Despite the fact that superficially the pictures of oscillations described in Refs. 1, 4 are similar, the distribution functions for the log conductivity are considerably different for the one dimensional and two dimensional cases. In the first case, the distribution function has a nonsymmetric form, with a "tail" extending toward the low-conductivity side, while in the second case the distribution function has a tail extending toward the high-conductivity side.

In this paper we investigate the distribution function for fluctuations in $\ln G(V_g)$ in a two-dimensional system.[3] The experimental data are compared with the results of a theoretical study of the statistical properties of mesoscopic fluctuations in the hopping conductivity of one-dimensional and two-dimensional systems.[5–8] The results of the paper suggest that the model consisting of a sum of individual chain conductivities is the more correct one to apply to these systems. In order to describe the experiments quantitatively we adopt a microscopic model of the hopping conductivity of a short channel which includes small-scale fluctuations of the charged impurity potential.

2. DISTRIBUTION FUNCTION OF THE LOG CONDUCTIVITY

In Ref. 5 a general expression was obtained for the distribution function over an ensemble of samples of the log conductivity of a randomly inhomogeneous barrier structure of finite area. The basic premise of this derivation was the following: because of spatial fluctuations in the barrier parameters, the total conductivity G is determined by

 0038-5646/89/121229-08$04.00

"punctures", i.e., rare regions with anomalously high conductivity. We denote the local conductivity of a puncture by $\tilde{G}\exp(-u)$ (where $\tilde{G}$ is a preexponential factor) and introduce a density of punctures $\rho(u)$ such that $\rho(u)du$ is the concentration of punctures whose log conductivity lies in the interval from $-u$ to $-u+du$ in a sample of infinite area. The distribution function of the log conductivity is expressed in terms of $\rho(u)$ as follows[5]:

$$f(Q)=\frac{e^{-Q}}{2\pi}\int_{-\infty}^{\infty}\exp\left\{ite^{-Q}+S\int_0^{\infty}\rho(u)\left[\exp\left(-\frac{itS_0e^{-u}}{S}\right)-1\right]du\right\}dt, \quad (1)$$

where

$$Q=-\ln(GS_0/\tilde{G}S), \quad (2)$$

S is the area of the barrier, and S_0 is a characteristic area of a puncture. Since the higher the conductivity the more rarely the punctures encounter each other, the function $\rho(u)$ can be cast in the form

$$\rho(u)=(1/S_0)\exp[-\Omega(u)], \quad (3)$$

with $\Omega(u)\gg 1$ and decreasing with increasing u. When (3) is substituted into (1), it is found that for a large enough area S the position of the maximum of the distribution function is determined by "optimal" punctures, i.e., those for which the derivative of $\exp[\Omega(-u)]\exp(-u)$ is a maximum. Let us denote the corresponding value of u by $u_{\rm opt}$. The criterion that the area S be sufficiently large then reduces to the condition $S\rho(u_{\rm opt})\gg 1$, which implies that the number of optimal punctures in a typical sample is much larger than unity. This condition can be cast in the form of a strict inequality $\nu>1$, where the parameter ν is defined as

$$\nu=\ln(S/S_0)/\Omega(u_{opt}). \quad (4)$$

For $\nu<1$ we do not find an optimal puncture in a typical sample. The position of the maximum of the distribution function (1) for $\nu<1$ is determined by the most conductive of the punctures which exist in a typical sample. The value $u=u_f>u_{\rm opt}$ corresponding to this puncture is found from the condition $S\rho(u_f)\sim 1$, which is equivalent to the condition

$$\Omega(u_f)=\nu\Omega(u_{opt}). \quad (5)$$

From this we see that u_f decreases as a function of ν for $\nu<1$. The expression for the distribution function for $\nu<1$ is easy to write down once we introduce the auxiliary function:

$$\varphi(\nu)=-\left.\frac{d\Omega}{du}\right|_{u=u_f(\nu)}. \quad (6)$$

It is easy to see that $\varphi(\nu)$ increases with increasing ν. For $\nu=1$ we have $u_f(1)=u_{\rm opt}$ and $\varphi(1)=1$, since $\Omega'_{u_{\rm opt}}=-1$. From this we see that the condition $\nu<1$ is equivalent to the condition $\varphi<1$. For $\nu<1$, Eq. (1) can be transformed to the form

$$f(Q)=\frac{e^{-\Delta}}{\pi}\int_0^{\infty}\exp\left[-x^{\varphi}\cos\left(\frac{\pi\varphi}{2}\right)\right]\cos\left(xe^{-\Delta}-x^{\varphi}\sin\frac{\pi\varphi}{2}\right)dx,$$

$$\varphi<1, \quad (7)$$

where

$$\Delta=Q-\nu\Omega(u_{opt})-u_f(\nu)+(1/\varphi)\ln[\Gamma(1-\varphi)/\varphi]$$

$$=-\ln(G/\tilde{G})-u_f(\nu)+(1/\varphi)\ln[\Gamma(1-\varphi)/\varphi], \quad (8)$$

and $\Gamma(t)$ is the gamma function. Using (7), we can calculate the average value Δ:

$$\langle\Delta\rangle=C(1/\varphi-1), \quad (9)$$

where $C=.577$ is the Euler-Mascheroni constant, and also the corresponding moments:

$$M_n=\langle(\Delta-\langle\Delta\rangle)^n\rangle=(-1)^n\zeta(n)(n-1)!(\varphi^{-n}-1),\ n=2,3,$$
$$M_4=\frac{\pi^4}{15}\left(\frac{1}{\varphi^4}-1\right)+\frac{\pi^4}{12}\left(\frac{1}{\varphi^2}-1\right)^2, \quad (10)$$

where $\zeta(n)$ is the zeta function.

Equations (7)–(10) become inapplicable in the region of values of φ close to unity, in particular for $1-\delta\leqslant[\Omega''(u_{\rm opt})]^{1/2}\ll 1$. The distribution function (1) has the form

$$f(Q)=\frac{1}{\pi w}\int_0^{\infty}\exp\left(-\frac{\pi x}{2}\right)\cos\left(x\frac{\Delta_1}{w}-x\ln x\right)dx \quad (11)$$

for $|1-\varphi|\ll(\Omega''(u_{\rm opt}))^{1/2}$, where

$$\Delta_1=Q-u_{opt}-\Omega(u_{opt})+\ln\left[\left(\frac{2\pi}{\Omega''(u_{opt})}\right)^{1/2}\Phi\left(\frac{1-\varphi}{[2\Omega''(u_{opt})]^{1/2}}\right)\right], \quad (12)$$

$$w^{-1}=\left(\frac{2\pi}{\Omega''(u_{opt})}\right)^{1/2}\exp\left[\frac{(1-\varphi)^2}{2\Omega''(u_{opt})}\right]\Phi\left(\frac{1-\varphi}{[2\Omega''(u_{opt})]^{1/2}}\right). \quad (13)$$

Here

$$\Phi(t)=\frac{1}{\pi^{1/2}}\int_t^{\infty}\exp(-x^2)dx$$

is the error function. It is clear from Eq. (11) that for $|1-\varphi|\ll(\Omega''(u_{\rm opt}))^{1/2}$ the distribution function is a universal function of the ratio Δ_1/w, while only its width depends on the parameter φ. In the interval $|1-\varphi|\sim(\Omega''(u_{\rm opt}))^{1/2}$ a constriction of the distribution function takes place. For $\Delta_1\gg w$ it falls off as $\exp[-\exp(\Delta_1/w)]$, while for $\Delta_1<0, |\Delta_1|\gg w$ it decreases more slowly, as w/Δ_1^2; i.e., as a power-law; therefore the average value of this distribution function diverges, along with its higher moments.

Equations (7) and (11) for the distribution function were obtained in Ref. 5 by averaging over all samples. It can be shown that the same distribution function applies to mesoscopic conductivity fluctuations in a single sample as the Fermi level varies. The proof of this assertion (i.e., the proof of ergodicity of the mesoscopic fluctuations) reduces to a proof of the fact that all the even-order correlation functions reduce to zero as the difference in arguments increases (see

Ref. 9). It is carried out in a way analogous to that described in Refs. 5, 7, 8, where the second-order correlator was calculated for a number of specific current-transport models.

3. EXPERIMENTAL RESULTS

Figure 1 shows an example of the experimental dependence on gate voltage of the conductivity of a GaAs field-effect transistor at several temperatures. The fabrication of the structure was described in Ref. 3. The length L of the conducting channel along the current direction was 4 μm, while its width Λ in the transverse direction was 200 μm (the thickness of the conducting channel was on the order of 200 Å). It is clear that, in addition to the fluctuations, there is a monotonic variation of the function $\ln G(V_g)$ associated with a decrease in the density of states as the Fermi level μ decreases. When we examine intervals of variation of V_g within whose limits the density of electron states can be considered to be approximately constant, we always find that they contain something like 4 or 5 oscillations. Now, it is plain that a good statistical analysis of mesoscopic conductivity fluctuations can be carried out only for a large number of oscillations. In order to check how informative such an analysis can be for this rather small number of oscillations, we analyzed our results by first using the model presented in Ref. 10 for hopping conductivity on a one-dimensional chain. It was important to clarify whether a distribution function obtained by investigating about five oscillations can reflect the basic features of the conductivity fluctuations of a one-dimensional system, and how the distribution function of the log conductivity depends on the number of oscillations included in the analysis.

Figure 2 shows the results of modeling the function $\ln G(\mu)$ given in Ref. 10. Processing of the data was carried out in the following fashion. We first broke up the total interval of variation of the argument μ into 125 to 600 points, each of which had its corresponding value of $\ln G(V_g)$. Then

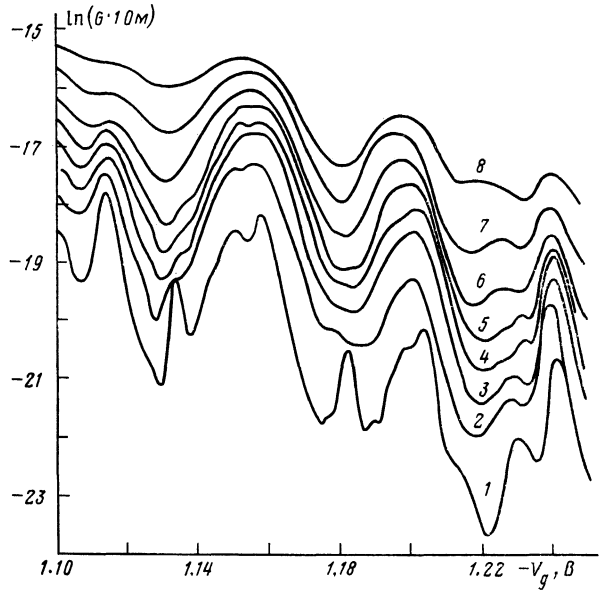

FIG. 1. Conductivity fluctuations in the channel of a GaAs FET at various temperatures T:1.5; 2.0; 2.5; 3.0; 3.5; 4.2; 6.0; 8.0 K (curves 1–8).

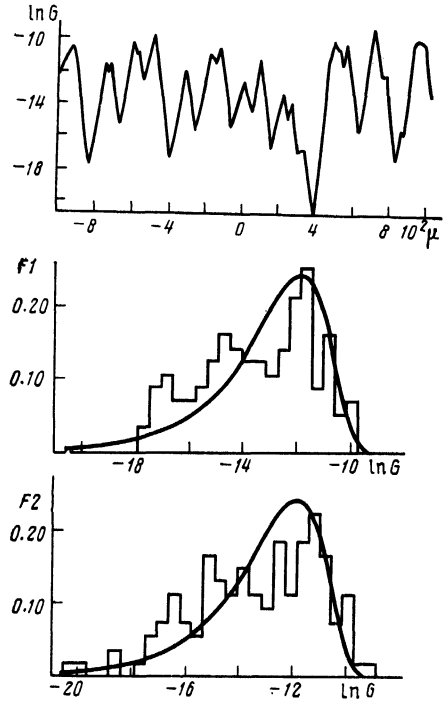

FIG. 2. Conductivity fluctuations of a one-dimensional chain of hops (results of the modeling in Ref. 10) and histograms of the distribution of the log conductivity obtained from an analysis of four oscillations ($F1$) and all the functions $\ln G(\mu)$ ($F2$).

we determined the fraction F of values of $\ln G(\mu)$ which fell into a given interval $[\ln G, \ln G + \delta]$. The interval δ was chosen to be 0.02 to 0.03 of the total range of variation of $\ln G$. Figure 2 shows histograms of $F(\ln G)$ obtained by analysis of the first four oscillations of the function $\ln G(\mu)$ ($F1$) and of all the curves containing $\approx$ 12 oscillations ($F2$). Despite the small number of oscillations analyzed in histogram $F1$ an asymmetry with a smooth falloff on the small-conductivity side is evident. Increasing the number of oscillations under study (i.e., $F2$) only smooths out the histogram and allows us to better study the tail of the distribution function. The same tendency is traceable as the number of oscillations included is increased further (we have analyzed the results of modeling the conductivity of a one-dimensional chain given in Ref. 11, which contained $\sim$70 oscillations). Let us note that the symmetry of the distribution function is difficult to see directly from the shape of the oscillations on the fluctuating curve $\ln G(\mu)$.

The theoretical expression for the distribution function of the logarithm of the hopping conductivity of a one-dimensional system has the form (7) with Δ replaced by $-\Delta$ and $\varphi(\nu)^{1/2}$ (Ref. 8). From the data presented in Fig. 2 the moments can be calculated: $M_2 = 5.5$, $M_3 = 6.9$, and $M_4 = 83$. The corresponding values of φ found from Eq. (10) come to 0.51, 0.65, and 0.57. The function (7) for $\varphi = 0.5$ is shown in Fig. 2 by the smooth curve; it is clear that this curve describes the modeling results satisfactorily. Therefore our processing of the data from Ref. 10 has verified that it is correct to carry out a statistical analysis of the mesoscopic conductivity fluctuations even when the number of oscillations is not large.

In contrast to the functions obtained in modeling, the experimental curves have a clearly visible overall monotonic variation (Fig. 1). This constitutes an additional obstacle to statistical processing of the data, which we overcome in the following way. The monotonic variation in $\ln G_0(V_g)$ at each temperature is extracted from the experimental functions by using the least-squares method to approximate it with a straight line. This line $\ln G_0(V_g)$ is then subtracted from the experimental curves. Once this is done, we follow the procedure described above to construct conductivity histograms $F(\ln[G(V_g)/G_0(V_g)])$ for each temperature. In Fig. 3 we show an example of these histograms obtained at three temperatures. In contrast to the distribution function for the one-dimensional case (Fig. 2), a smoother falloff of the histogram is observed on the side of large conductivities. It is also clear that the width of the histogram decreases with increasing temperature, which is a consequence of the decreasing amplitude of oscillation. The values of the second moment M_2 for the fluctuating function $\ln[G(V_g)/G_0(V_g)]$ come to 0.97 for $T=1.5$ K, 0.54 for $T=4.2$ K and 0.11 for $T=8$ K. The corresponding values of φ determined by using Eq. (10) equal 0.79, 0.89, and 0.97. At those values of φ which are close to unity, the distribution function is described by Eq. (11) and depends only on the argument $\Delta_1/w(\varphi)$. Therefore the experimental histograms for all eight temperatures are approximated by the same function (11), in which the parameter $w(T)$ is determined each time by minimizing the mean-square deviation of the theoretical curve from the experimental histogram. The results of this analysis for three temperatures are shown by the smooth curve in Fig. 3.

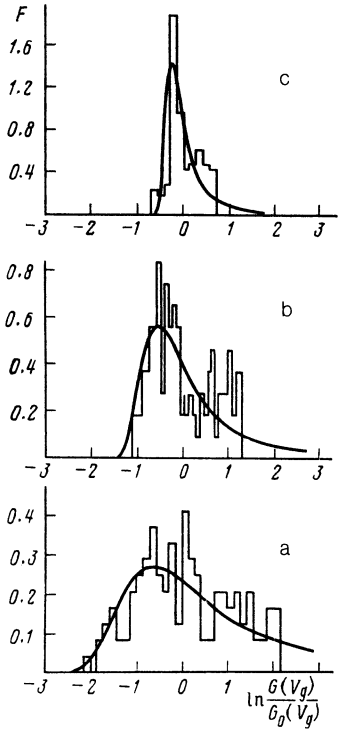

FIG. 3. Histogram of the distribution of the log conductivity of the experimental dependences for the three temperatures 1.5 (a), 4.2 (b) and 8 K (c) (curves 1,6 and 8 of Fig. 1) after subtracting the monotonic part from them. The smooth curves show the corresponding approximating functions.

Because of the small number of oscillations on the $\ln[G(V_g)/G_0(V_g)]$ curves being processed, considerable scatter can be observed in the histograms. In order to decrease it, we carried out the following procedure. All eight of the histograms were reduced to the same temperature $T=1.5$ K by compressing the ordinate and expanding the abscissa by a factor of $w(1.5)/w(T)$. Then the histograms were shifted along the abscissa until the maxima of the corresponding approximate curves (11) coincided. A histogram was then constructed by taking the arithmetic average of the individual histograms which were transformed using the methods described above. This histogram is shown in Fig. 4, together with the theoretical distribution function (11). Despite the fact that perfect scaling of the picture of the oscillations as the temperature is varied does not occur (see Fig. 1), this averaging procedure leads to a considerable decrease in the scatter. It is clear that agreement between theory and experiment is satisfactory. The analysis leads us to the conclusion that the system under study is a two-dimensional array of parallel-connected random conducting paths. The question of the microscopic structure of these paths will be discussed in the following section.

4. DISCUSSION

As we indicated in Sec. 2, the form of the distribution function of a short sample is universal, and gives no information about the microscopic mechanism of the current transport. On the other hand, the width of the distribution function w and the position of its maximum $\ln G_m$ depend on the specific current transport model. Both these quantities are determined from the experimental histograms at eight temperatures. In order to analyze quantitatively the functions $\ln G_m(T)$ and $w(T)$ obtained in this way it is necessary to adopt a specified model of the hopping conductivity.

A first glance suggests that the model of an amorphous film proposed in Ref. 12 ought to be a good candidate. In this model it is assumed that current transport across an amor-

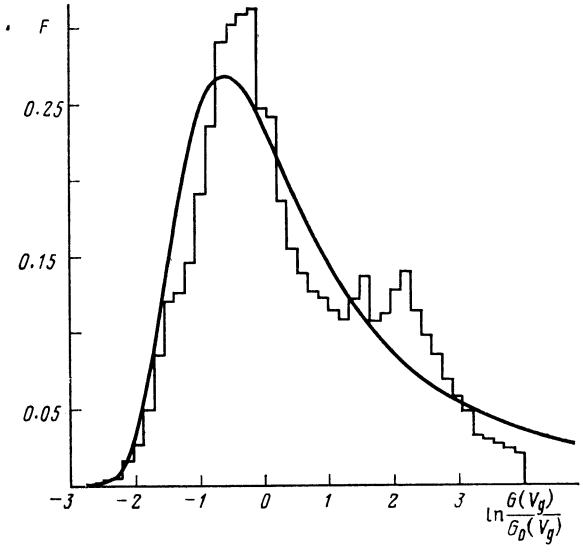

FIG. 4. Histogram resulting from averaging over the data reduced to $T=1.5$ K for eight temperatures, and the corresponding theoretical distribution function of the log conductivity.

phous film of thickness L comes about by hopping of electrons along localized states whose radius of localization a is assumed to be constant, while the density of states g does not depend on energy. For sufficiently small thicknesses L extended, almost equivalent chains of impurities are responsible for the transverse conductivity of a large-area film. Using simple considerations,[13] we can find the mean position ε of the band near the Fermi level in which the energy levels of these impurities are located and find the number of links N in the chain. Let us denote by v_0 the small volume in which an impurity should fall in order to become a link of the chain. Then the probability of forming a chain is $P_N = (gv_0\varepsilon)^N$. The conductivity of a single link of the chain equals $\tilde{G}\exp[-(2L/aN+\varepsilon/T)]$ and is determined by the probability of tunnelling of an electron over a distance L/N and by activation over a characteristic energy ε. The contribution to the conductivity of the film of chains with a given N and ε has the form

$$G_N \propto (g\varepsilon v_0)^N \exp\left[-\frac{2L}{aN}-\frac{\varepsilon}{T}\right]. \tag{14}$$

The quantity G_N is a maximum for

$$\varepsilon = NT \text{ и } N=[2L/a\lambda]^{1/2}, \tag{15}$$

where

$$\lambda=\ln(a^{1/2}/gTv_0L^{1/2}). \tag{16}$$

Substituting N, ε into Eq. (14), we find for the specific conductivity (i.e., the conductivity per unit volume) of the film

$$\ln[GS_0/\tilde{G}S]=-2[2L\lambda/a]^{1/2}. \tag{17}$$

Equation (17) is valid for $\lambda \gg 1$.

Let us try to compare the experimental results with the predictions of this model of an amorphous film. From Eq. (17) there follows the relation

$$d\ln G/d(1/T)=\varepsilon=NT. \tag{18}$$

Let us study the experimental behavior of the quantity $d\ln G/d(1/T)$. In Fig. 5 we show the temperature dependence of the sample conductivity for various values of V_g, which correspond to V_g = const cross-sections of the curves in Fig. 1. At small values of $|V_g|$, for which multiple electron hopping gives a contribution to the conductivity of the sample, the temperature dependence of the conductivity has a curvature which is characteristic of variable-range hopping. The activation energy in this regime decreases as the temperature decreases (curves 1, 2). In the region of large fluctuations, the behavior of the conductivity can be described by a single activation energy, whose value undergoes mesoscopic fluctuations as we pass from one peak to the other in Fig. 1 (curves 3–6). In addition, curve 7 exhibits a substantial change in slope as the temperature varies.

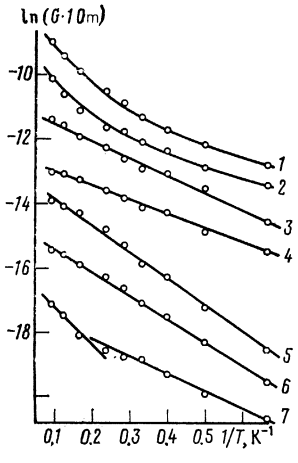

FIG. 5. Temperature dependence of the channel conductivity for various values of $|V_g|$: 1—1.105; 2—1.117; 3—1.148; 4—1.157; 5—1.195; 6—1.200; and 7—1.241 V (curves 1–6 are arbitrarily shifted along the ordinate axis).

In the temperature interval under study here, the activation energy of the curves in Fig. 5, ignoring their difference in shape, varies from 0.4 meV to 0.8 meV. At the lowest temperature $T = 1.5$ K we obtain from (18) a value for N of 3 to 6. For $L = 4\ \mu$ and $a = 100$ Å this value of N can be obtained only for an anomalously large $\lambda \approx 50$, while according to (16) the quantity λ does not exceed unity. (For this estimate the volume v_0 was set equal to 10^{-18} cm^{-3}, the width of the impurity band set equal to 10 meV, and the concentration of donors set equal to 10^{17} cm^{-3}; these numbers imply a value of the density of states $g \approx 10^{19}$ cm$^{-3}\cdot$eV^{-1}.)

It is our view that the inapplicability of the amorphous-film model to the system under study is connected with the fact that the channel of a GaAs transistor consists of a layer of heavily-doped semiconductor. For such a structure, the region of values of V_g in which strong conductivity fluctuations are observed corresponds to electron concentrations in the channel which are too small to screen fluctuations in the charged donor potential which occur in the region surrounding the conducting channel.[14] These fluctuations in the charged donor potential then cause the distribution of electrons to become quite inhomogeneous. The contour of the bottom of the conduction band consists of a set of potential barriers of varying heights and all possible spatial scales, with filled electron states located in the regions between the barriers. The passage of current comes about by tunnelling-mediated electron hops through these barriers. The height of a typical barrier $\delta(R)$ caused by fluctuations in the donor concentration on a scale R can be estimated in the following fashion.[15] A typical fluctuation in the number of charged donors in a sphere of radius R is $(N_d R^3)^{1/2}$, where N_d is the mean concentration of donors. The potential caused by this charge fluctuation has the form

$$\gamma(R)=(e^2/\varkappa)\,[N_dR]^{1/2}, \tag{19}$$

where $\varkappa$ is the dielectric permittivity. The height of the barrier $\delta(R)$ increases with increasing R up to a scale R_c (the radius of nonlinear screening) determined by the condition that the excess fluctuation charge in a volume R_c, equal to $(N_dR_c^3)^{1/2}$, begins to be balanced by the electron charge nR_c^2 in the channel which screens the appearance of the potential fluctuation. From this we obtain

$$R_c=N_d/n^2 \tag{20}$$

and for the corresponding value of the potential amplitude we have

$$\gamma(R_c)=\gamma_c=e^2N_d/\varkappa n. \tag{21}$$

The tunnelling transparency D of a barrier of height δ_c and thickness R_c is

$$|\ln D| = (m\gamma_c)^{1/2} R_c/\hbar = N_d^{3/2}/n^{5/2} a_B^{1/2}, \quad (22)$$

where m is the electron mass, and $a_B = \hbar\varkappa/me^2$ is the Bohr radius.

It is clear from this expression that as the concentration n is decreased by increasing $|V_g|$, the transparency of a typical barrier drops sharply. Therefore, in a sample whose width Λ considerably exceeds the length L, a certain point is reached at which the conductivity is determined by rare "grooves" between the contacts, along which the amplitude of the potential contour is considerably smaller than a typical value of δ_c. This concept is the basis of our model of current transport in a short sample with an inhomogeneous distribution of localized states.

Let us estimate the probability P_0 of forming a groove which links the transistor source and drain within which the height of the fluctuating contour is less than a certain value $\delta_0 \ll \delta_c$. The required probability equals the probability that potential fluctuations are absent over the entire length L of the conducting channel for all spatial scales which exceed a certain scale $R_0 \ll R_c$ determined by the condition $\delta(R_0) = \delta_0$. Let us surround this groove with a sphere of fixed radius R such that $R_0 \ll R \ll R_c$. The probability that the potential fluctuation is less than δ_0 in a given sphere is $\delta_0/\delta(R)$, where $\delta(R)$ is the typical value of the fluctuation (19). However, the probability that a potential fluctuation is less than δ_0 in all of the L/R spheres which are located along the channel length equals

$$P(R) = \left[\frac{\gamma_0}{\gamma(R)}\right]^{L/R} = \exp\left[-\frac{L}{R}\ln\left(\frac{\gamma(R)}{\gamma_0}\right)\right]. \quad (23)$$

In order to estimate the required probability P_0 we must multiply the quantities $P(R)$ for all scales R over which the fluctuations can be considered independent (for example, $R = R_0, 2R_0, 4R_0$, etc.). Since $|\ln P(R_k)|$ falls rapidly as the index k increases ($R_k = 2^k R_0$), the quantity P_0 coincides to exponential accuracy with $P(R_0)$, i.e.,

$$P_0 = P(R_0) = \exp(-L/R_0). \quad (24)$$

The potential contour along the axis of the groove consists of a series of barriers of heights on the order of $\delta(R_0)$ and thickness R_0. The order of magnitude of the tunnelling transparency of each of these barriers is $\exp\{-R_0[m\delta(R_0)]^{1/2\hbar^{-1}}\}$. If we assume the value of the transparency $D = \exp(-u)$ and express R_0 in terms of u by using (19), then the value of P_0 will be proportional to the puncture density $\rho(u)$ (Sec. 2). In this case we obtain for the logarithm of the puncture density

$$\Omega(u) = 5(Q_0/9)^{9/5}(4/u)^{4/5}, \quad (25)$$

$$Q_0 = \beta(L/a_B)^{5/9}(N_d a_B^3)^{1/9}, \quad (26)$$

where β is an unknown numerical coefficient, while the coefficient in (25) is introduced in such a way that the maximum of the product $\exp[-\Omega(u)]\cdot\exp(-u)$ equals $\exp(-Q_0)$. In this case, according to the universal scheme of Sec. 2, the quantity $-Q_0$ is the logarithm of the specific conductivity of a sample of infinite width. Comparing Eqs. (22) and (26), we see that the conductivity of the sample will be determined by the punctures when the condition

$$Q_0 \ll N_d^{3/2} n^{-5/2} a_B^{-1/2}$$

is fulfilled, i.e., when a sufficiently low concentration of electrons exists in the channel.

We remark that the quantity Q_0 does not depend on n. This comes about because in calculating the probability of forming punctures only the small scales $R \sim R_c$ turn out to be important, while the concentration of electrons n is determined by larger scales on the order of R_c.

Let us take note of a peculiarity of this model which distinguishes it from other models of inhomogeneous barriers in which the sample conductivity is determined by punctures. In all such models (e.g., in the amorphous film model) a puncture arises in the strong-fluctuation regime, where the concentration of impurities significantly exceeds its mean value. In the puncture model under discussion here, however, a puncture is created where the fluctuations are much smaller than the typical value, i.e., in the weak-fluctuation regime.

Let us attempt to apply our model to the experimental situation. First of all, we note that Eq. (26) does not depend on temperature. This is related to the fact that in deriving Eqs. (25), (26) it was assumed that the energy of the localized states between which the tunnelling occurs are the same, and does not differ from the Fermi level. The scatter of these energy levels which exists in reality leads to the appearance of a finite activation energy ε and correspondingly to a correction ε/T to the value of Q_0 in Eq. (26). In what follows, we will see that this correction is small. Therefore, we will assume that Eq. (25) for $\rho(u)$ remains valid, and that we need only substitute the modified value

$$Q_0(T) = \beta(L/a_B)^{5/9}(N_d a_B^3)^{1/9} + \varepsilon/T \quad (27)$$

into it.

In Sec. 2 we presented expressions for the width and position of the maximum of the distribution function for the log conductivity, both expressed in general form in terms of the function $\Omega(u)$. Let us calculate the quantities which enter into these expressions within the framework of the model under discussion here. Substituting Eq. (25) into (4), (5), and (6), we obtain

$$u_{opt} = {}^4/_9 Q_0, \quad (28)$$

$$\nu = ({}^9/_5 Q_0)\ln(\Lambda/\Lambda_0), \quad (29)$$

$$u_f(\nu) = {}^4/_9 Q_0/\nu^{5/4}, \quad (30)$$

$$\varphi(\nu) = \nu^{9/4}, \quad (31)$$

where Λ_0 is the characteristic width of the groove. Furthermore, in Eqs. (12) and (13) there figures the quantity $\Omega''(u_{\rm opt}) = 81/(20Q_0)$. Substituting it into (12) and (13), and also using (31), we obtain for the width of the distribution function

$$w^{-1} = ({}^5/_8 Q_0)^{1/2}\exp[{}^5/_8 Q_0(1-\nu)^2]\cdot\Phi((1-\nu)({}^5/_8 Q_0)^{1/2}), \quad (32)$$

while for the position of the maximum

$$\ln G_m = \ln(\tilde{G}\Lambda/\Lambda_0) - Q_0 - 0.2w + \ln\{({}^5/_8\pi Q_0)^{1/2}\Phi((1-\nu)({}^5/_8 Q_0)^{1/2})\}, \quad (33)$$

where G is the total conductivity of the sample.

Our goal is to compare the values of the width calculated using Eq. (32) with the experimental values obtained from an analysis of the histograms. In order to do this, we proceed in the following way. Let us pick the value $\Lambda_0 \approx a_B = 100$ Å. Using for $\tilde{G}$ the theoretical estimate $g = e^2T/\tau_{ph}$,[15] so that $G = 1.1 \cdot 10^{-4}\ \Omega^{-1}$ for $T = 1.5$ K and $\tau_{ph}^{-1} \approx 10^{11}\text{sec}^{-1}$, and Eqs. (29), (32), and (33) for ν, $\ln G_m$, w^{-1}, we can now determine the values of the parameters ν, Q_0 and w for each temperature. To do this, we substitute the experimental values of $\ln G_m(T)$ into the system of three equations (29), (32) and (33), where these values are found by shifting the maxima of the approximate distribution functions relative to the mean value $\ln G_0(T)$. In place of the mean value of the log conductivity for each temperature we use the value of $\ln G_0(V_g)$ at that value of V_g which corresponds to the middle of the interval of variation of V_g in Fig. 1.

The parameters w and Q_0 obtained in this way are shown in Fig. 6 along with the experimental values of w. It is clear that in the low-temperature region we find adequate agreement between the theoretical and experimental values of $w(T)$. In the region $T \geqslant 4$ K, we observe experimentally a stronger decrease in the width of the distribution function with temperature than is predicted by theory. We note that there is some arbitrariness in our choice of the parameter $\tilde{G}$; however, increasing its value by a factor of 10 causes the calculated values of $w(T)$ to increase by approximately 30% (curve 2 in Fig. 6).

Let us now discuss the values of Q_0 obtained in this way (Fig. 6). It is clear that in the interval 1.5 to 8 K these values vary from 22 to 17. Within the framework of our model, the quantity $Q_0(T)$ is determined by Eq. (27). The characteristic value of the activation energy ε, which is determined by the slope of the function $Q_0(T)$, comes to $\varepsilon \approx 1$ meV. From this we see that the value of the activation correction to Q_0, which equals ε/T, amounts to $(0.1\text{–}0.3)Q_0$ in the temperature interval under investigation. If we compare the value of Q_0 at $T = 6$ K with the theoretical value (26), we obtain the value 0.9 for the coefficient β for $N_d = 4 \cdot 10^{16}\ \text{cm}^{-3}$.

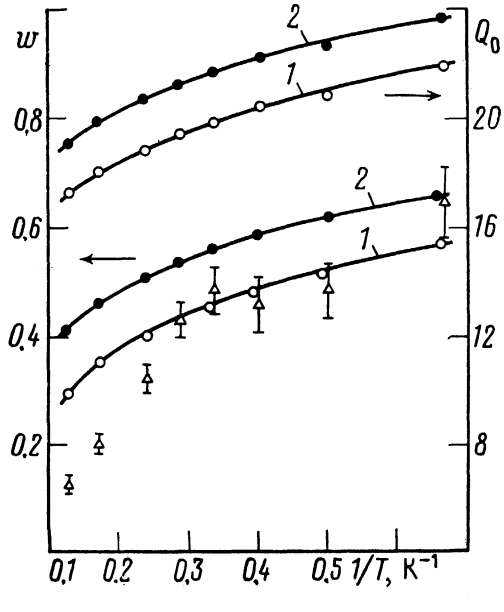

FIG. 6. Temperature dependence of the experimental value of the width w of the distribution function and the calculated parameters w and Q_0 for two values of the frequency τ_{ph}^{-1}: $10^{11}\ \text{sec}^{-1}$ (curve 1) and $10^{12}\ \text{sec}^{-1}$ (curve 2).

We noted above that our model of the current transport is applicable when the conductivity $G \approx \tilde{G}\exp(-Q_0)$ of the punctures exceeds the conductivity arising from tunnelling through a typical barrier in the potential contour, i.e., when the condition

$$Q_0 \ll |\ln D| = N_d^{3/2} n^{-5/2} a_B^{-3/2}$$

is fulfilled [Eq. (22)]. Let us estimate the initial concentration n_c of electrons for which this condition is fulfilled. For $Q_0 = 20$ we obtain $n_c \approx 5 \cdot 10^{10}\ \text{cm}^{-2}$. The results of capacitance measurements[3,14] suggest that strong fluctuations in $\ln G(V_g)$ are observed for $n \lesssim 4 \cdot 10^{10}\ \text{cm}^{-2}$; this density coincides in order of magnitude with the estimate given here.

From this we see that, on the whole, a model based on current transport determined by hopping of electrons along paths with anomalously low potential contour barriers gives a satisfactory description of the relation between mean conductivity and the amplitude of fluctuations at various temperatures. The specific mechanism for the conductivity fluctuations as V_g varies is the same in this model as in the model of an amorphous film.[7] As V_g varies, so does the position of the Fermi level. This leads to a variation in the effective activation energy for all the hops, and to an exponentially strong decrease in the resistance corresponding to them. For $\nu < 1$ the resistance of a sample is determined by the maximum resistance of the most conducting chain. As the position of the Fermi level varies there are sudden changes both in the maximum resistance within a single chain and in the particular chains which determine the conductivity of the sample. Because of the exponential scatter of individual resistances, these sudden changes lead to fluctuations in the sample conductivity; the minimum conductivity corresponds to the instant at which the chains are switched.

An exponential variation in the value of each of the resistances also takes place as the temperature is raised. As in the model of an amorphous film, this should lead to conductivity fluctuations with a characteristic "period" $\delta T \sim T^2/\varepsilon$. We could consider the kink in the temperature dependence of the conductivity (curve 7 of Fig. 5) an example of such fluctuations, which can be interpreted as a switching-on of resistance with different activation energies. However,for experimental values of the activation energy $\varepsilon = 0.4$ to 0.8 meV, the period δT at $T = 4$ K should come to approximately 2K, i.e., in the temperature interval under discussion we should see 2 to 3 fluctuations in the curve of $\ln G(T)$ for each V_g. However, the majority of curves in Fig. 5 do not exhibit kinks. The reason for this remains unexplained.

In conclusion, let us discuss the observed deviations of the experimental function $w(T)$ from theory in the high-temperature region (Fig. 6). The reason for this may be related to the fact that as the temperature is increased a transition should occur from the regime of chainlike conduction to a regime where the sample conductivity is determined by a rather small number of regions having the form of branched clusters. In this case, the increase in the number of conducting paths which takes place leads to an enhancement in the attenuation of the fluctuation amplitude and to a sharp de-

crease in the width of the distribution function of the log conductivity.

We are grateful to E. I. Laiko for his help in carrying out the experiments. We also thank B. I. Shklovskii for making a number of useful comments after reading the manuscript of the article.

[1] A. B. Fowler, A. Harstein, and R. A. Webb, Phys. Rev. Lett. **48**, 196 (1982).
[2] R. A. Webb, A. B. Fowler, A. Harstein, and J. J. Wainer, Surf. Sci. **170**, 14 (1986).
[3] A. O. Orlov, A. K. Savchenko, E. V. Chenskii *et al.*, Pis'ma Zh. Eksp. Teor. Fiz. **43**, 421 (1986) [JETP Lett. **43** 540 (1986)].
[4] E. I. Laiko, A. O. Orlov, A. K. Savchenko *et al.*, Zh. Eksp. Teor. Fiz. **93**, 2204 (1987) [Sov. Phys. JETP **66**, 1258 (1987)].
[5] M. E. Raikh and I. M.Ruzin, Zh. Eksp. Teor. Fiz. **92**, 2257 (1987) [Sov. Phys. JETP **65**, 1273 (1987)].
[6] R. A. Serota, R. K. Kalia, and P. A. Lee, Phys. Rev. **B33**, 8441 (1986).
[7] M. E. Raikh and I. M. Ruzin, Fiz. Tekh. Poluprovod. **22**, 1262 (1988) [Sov. Phys. Semicond. **22**, 799 (1988)].
[8] M. E. Raikh and I. M. Ruzin, Zh. Eksp. Teor. Fiz. **95**, 1113 (1989) [Sov. Phys. JETP **68**, 642 (1989)].
[9] P. A. Lee and A. D. Stone, Phys. Rev. Lett. **55**, 1622 (1985).
[10] P. A. Lee, Phys. Rev. Lett. **48**, 2042 (1984).
[11] J. Yu and R. A. Serota, Phys. Rev. **40**, 1989.
[12] M. Pollak and J. J. Hauser, Phys. Rev. Lett. **31**, 1304 (1973).
[13] A. V. Tartarovskii, M. V. Fistul', M. E. Raikh, and I. M. Ruzin, Fiz. Tekh. Poluprovod. **21**, 603 (1987) [Sov. Phys. Semicond. **21**, 370 (1987)].
[14] A. O. Orlov, A. K. Savchenko, and V. I. Shklovskii, Fiz. Tekh. Poluprovod. **23**, 1334 (1989) [Sov. Phys. Semicond. **23**, 830 (1989)].
[15] B. I. Shklovskii and A. L. Efros, *Elektronnye svoistva legirovannykh poluprovodnikov* (*Electronic Properties of Doped Semiconductors* Springer, New York, 1987); Nauka, Moscow, 1979.

Translated by Frank J. Crowne